Heterogeneity of fibrillin-rich microfibrils extracted from human skin of diverse ethnicity

DOI:
10.1111/joa.13217

Document Version
Accepted author manuscript

Heterogeneity of fibrillin-rich microfibrils extracted from human skin of diverse ethnicity

Short title: Fibrillin rich microfibrils and skin ethnicity

Abigail K Langton[1,2]; Mark Hann[3]; Patrick Costello[1,2]; Poonam Halai[1,2]; Sabrina Sisto Alessi César[4]; Anna Lien-Lun Chien[4]; Sewon Kang[4]; Christopher E M Griffiths[1,2]; Michael J Sherratt[5] and Rachel E B Watson[1,2]

[1]Centre for Dermatology Research, The University of Manchester & Salford Royal NHS Foundation Trust, Manchester Academic Health Science Centre, UK;

[2]NIHR Manchester Biomedical Research Centre, Manchester University NHS Foundation Trust, Manchester Academic Health Science Centre, UK;

[3]Centre for Biostatistics, The University of Manchester, Manchester Academic Health Science Centre, UK;

[4]Department of Dermatology, Johns Hopkins University School of Medicine, Baltimore, Maryland, USA;

[5]Division of Cell Matrix Biology and Regenerative Medicine, The University of Manchester, UK.

CORRESPONDING AUTHOR:

Dr Abigail Langton, 1.726A Stopford Building, Oxford Road, Manchester, M13 9PT, UK;

Tel: 44 (0)161 275 1149, Fax: 44 (0)161 275 5382;

E-mail: abigail.langton@manchester.ac.uk

ABSTRACT

The dermal elastic fibre network is the primary effector of skin elasticity, enabling it to extend and recoil many times over the lifetime of the individual. Fibrillin-rich microfibrils (FRMs) constitute integral components of the elastic fibre network, with their distribution showing differential deposition in the papillary dermis across individuals of diverse skin ethnicity. Despite these differential findings in histological presentation, it is not known if skin ethnicity influences FRM ultrastructure. FRMs are evolutionarily highly conserved from jellyfish to man, and regardless of tissue type or species, isolated FRMs have a characteristic 'beads-on-a-string' ultrastructural appearance with an average inter-bead distance (or periodicity) of 56 nm. Here, skin biopsies were obtained from the photoprotected buttock of healthy volunteers (18-27 years; African: n=5; European: n=5) and FRMs were isolated from the superficial papillary dermis and deeper reticular dermis and imaged by atomic force microscopy. In the reticular dermis there was no significant difference in FRM ultrastructure between European and African participants. In contrast, in the more superficial papillary dermis, inter-bead periodicity was significantly larger for FRMs extracted from European participants than from African participants by 2.20 nm ($P<0.001$). We next assessed whether these differences in FRM ultrastructure were present during early post-natal development by characterizing FRMs from full-thickness neonatal foreskin. Analysis of FRM periodicity identified no significant difference between neonatal cohorts ($P=0.865$). This data suggests that at birth, FRMs are developmentally invariant. However, in adults of diverse skin ethnicity, there is a deviation in ultrastructure for the papillary dermal FRMs, that may be acquired during the passage of time from child to adulthood. Understanding the mechanism by which this difference in papillary dermal FRMs arises warrants further study.

KEY WORDS

Fibrillin-rich microfibrils, skin ethnicity, extracellular matrix, atomic force microscopy.

ABBREVIATIONS

AFM, atomic force microscopy; DEJ, dermal-epidermal junction; ECM, extracellular matrix; FRM, fibrillin-rich microfibrils; NO, nitric oxide; ROS, reactive oxygen species; UVR, ultraviolet radiation.

REPRODUCED MATERIAL

All information and materials in the manuscript are original.

COMPETING INTERESTS

The authors declare no conflict of interest.

DATA SHARING

The data that support the findings of this study are available from the corresponding author upon reasonable request.

INTRODUCTION

Human skin has the crucial roles of maintaining homeostasis, defending against environmental insults, such as exposure to ultraviolet radiation (UVR) and protecting against external mechanical trauma, via the reversible deformation of its structure (Edwards and Marks, 1995). It is primarily composed of three main layers – an outermost cell-rich epidermis, an underlying dermis and the innermost hypodermis. Within the dermis, a complex extracellular matrix (ECM) consisting of collagens, elastic fibres, proteoglycans and glycosaminoglycans work in concert to imbue skin with its biomechanical properties. Components of the elastic fibre network - consisting of elastin, fibrillin-rich microfibrils (FRMs) and microfibril-associated proteins - are the primary effectors of elasticity, enabling the skin to extend and recoil many times over the lifetime of the individual (Hussain et al., 2013, Kielty et al., 2002). FRMs are evolutionarily highly conserved from jellyfish to man, which confirms their critical biomechanical importance (Kielty et al., 2002) and regardless of tissue type or species, isolated FRMs have a characteristic 'beads-on-a-string' ultrastructural appearance with an average inter-bead distance (or periodicity) of 56 nm (Keene et al., 1991).

The elastic fibre network forms a distinctive, highly ordered arrangement within the dermal ECM: at the dermal-epidermal junction (DEJ), superficial oxytalan fibres consist of candelabra-like cascades of discrete FRM bundles. These oxytalan fibres coalesce with a fine network of elastin- and fibrillin-rich elaunin fibres within the papillary dermis whilst in the reticular dermis, mature elastic fibres run in parallel to the DEJ (Cotta-Pereira et al., 1976, Afzal et al., 2017). Perturbations to the precise arrangement of elastic fibres readily leads to skin laxity (Langton et al., 2017) and clinical signs of ageing (Watson et al., 1999); loss of FRMs at the DEJ, accompanied by the deposition of disorganized elastotic material in the reticular dermis, has previously been shown to severely affect skin elasticity (Langton et al.,

2017, Langton et al., 2019b). Similarly, truncation and depletion of FRMs at the DEJ is characteristic of early photoageing and arises due to chronic sun exposure in Northern European populations (Watson et al., 1999). In contrast to white Northern Europeans, individuals of black African ancestry have a markedly different dermal ECM composition (Girardeau et al., 2009, Girardeau-Hubert et al., 2012, Langton et al., 2014). In young, healthy photoprotected skin, FRMs are differentially deposited in the papillary dermis, with black African skin containing significantly more FRMs than white Northern European skin (Langton et al., 2014). Furthermore, FRMs of black skin are much less susceptible to the remodelling events that arise following long-term exposure to UVR, as compared to white Northern European skin (Langton et al., 2019a). Despite these differential findings in histological presentation and skin elasticity, it is not known if skin ethnicity also influences FRM ultrastructure. Here, we present novel data characterizing the ultrastructure of FRMs isolated from the papillary and reticular dermis using human skin obtained from cohorts of black African and white Northern European ancestry.

METHODS

Skin biopsy procurement

Young healthy black African (mean age ± SD: 21.2 years ± 1.9; men: n = 2; women: n = 3; Fitzpatrick skin type (FST) VI) and white Northern European (22.4 years ± 2.3; men: n = 2; women: n = 3; FST I-II) volunteers were recruited to the study. Local ethical approval was obtained from the North West Research Ethics Committee (ref. 09/H1006/23) and the University of Manchester Research Ethics Committee (ref. 14161). Basic demographic information was collected and participants were asked to self-declare their ethnicity. Six mm diameter punch biopsies were obtained from photoprotected buttock under 1% lignocaine local anaesthesia. At the time of procurement, biopsies were bisected, snap frozen in liquid nitrogen and stored at -80 C.

Neonatal foreskins were obtained from black African-American (n = 5; FST VI) and white European American (n=4; FST I-II) infants following routine circumcision. Local ethical approval was obtained from The Johns Hopkins Institutional Review Board. All studies were conducted in accordance with the Declaration of Helsinki Principles with written, informed consent.

Fibrillin microfibril isolation

Fibrillin-rich microfibrils were isolated from the papillary dermis of adult buttock skin by cryosectioning bisected 6 mm skin biopsies *en face* to a depth of 400 µm. Next, 100 µm was cryosectioned from the skin biopsy and discarded. Fibrillin-rich microfibrils were then isolated from the remaining reticular dermal fraction of the skin biopsy (Figure 2a). Papillary and reticular dermal fractions were digested overnight in 0.5 mg/mL bacterial collagenase type IA (suspended in 0.4 M NaCl, 0.05 M Tris–HCl, 0.01 M $CaCl_2$ at pH 7.4, and

supplemented with protease inhibitors: 2 mM phenylmethanesulfonyl fluoride and 5 mM N-Ethylmaleimide). For the isolation of FRMs from neonatal foreskins, samples were finely minced and digested overnight in 0.5 mg/mL bacterial collagenase type IA. Extracts were subsequently purified by low pressure size-exclusion chromatography on an ÄKTA prime plus system coupled to a Sepharose CL-2B column (GE Healthcare, Little Chalfont, UK) which was equilibrated in high salt buffer (0.4 M NaCl, 0.05 M Tris–HCl at pH 7.4). FRMs were eluted from the column in the excluded volume (V_0) peak.

Atomic force microscopy and data processing

Fibrillin-rich microfibril ultrastructure was characterized by atomic force microscopy (AFM). Using the Multimode 8 AFM (Bruker AFM Probes, Camarillo, California USA) fitted with ScanAsyst-Air cantilevers, randomly selected 10 x 10 µm locations were scanned at a rate of 1.97 Hz. The morphologic metrics assessed were the number of beads per FRM and inter-bead periodicity. Periodicity was determined by measuring the distance between individual beads (n = 1000 for adult samples; n = 250 for foreskin samples) using WSxM scanning probe microscopy software and by routines written in Microsoft Visual Basic 6.0. Inter-bead periodicity is a widely used, reliable and quantitative marker for analysis of FRM ultrastructure (Eckersley et al., 2018, Hibbert et al., 2015, Sherratt et al., 2010).

Immunohistochemical staining

For immunohistochemical methodologies, skin biopsies were cryosectioned at 7 µm in a single run, using the same blade and cryostat settings. Biopsies were aligned perpendicular to the cryostat blade, with the dermis always sectioned through first. Immunofluorescence staining for FRMs (clone 11C1.3; dilution 1:100; ThermoFisher Scientific, Runcorn, UK) and fibrillin-2 (clone 48; dilution 1:100; Millipore (U.K.) Limited) were performed by fixation of

cryosections in 4% (w/v) paraformaldehyde (PFA) in phosphate-buffered saline. Primary antibody was applied at room temperature for 1 hour. Sections were then washed in TBS prior to incubation using the VectaFluor™ Excel Amplified DyLight® 594 Anti-Mouse IgG Kit (Vector Laboratories, Peterborough, U.K.). Dual immunofluorescence staining was performed to detect FRM and elastin (catalogue # AB2043; dilution 1:100; Millipore (U.K.) Limited, Feltham, U.K.) using the reagents and protocol from the VectaFluor Duet Immunofluorescence Double Labelling Kit (Vector Laboratories). Cryosections were fixed in 4% PFA, and hydrated in Tris-buffered saline. Primary antibodies were applied and maintained at a temperature of 4°C overnight. VectaFluor™ Duet Reagent [DyLight® 488 Anti-Rabbit IgG and DyLight®594 Anti-Mouse IgG cocktail (rabbit-green, mouse-red)] was applied for 30 minutes. Cell nuclei were visualized using 4',6-diamidino-2-phenylindole (DAPI).

Epidermal melanin was assessed in 7 µm cryosections using the modified Warthin-Starry procedure (Joly-Tonetti et al., 2016). Components of the Warthin-Starry developer solution (2% silver nitrate, 5% gelatin, 0.15% hydroquinone; Sigma-Aldrich) were prepared using acidulated water (distilled water adjusted to pH 3.2 using 1% aqueous citric acid) and pre-warmed to 54°C. Cryosections were fixed in acetone for 5 min and rinsed in acidulated water. Immediately prior to use, developer solution was prepared by thoroughly mixing 41.5 ml 2% silver nitrate, 103.5 ml 5% gelatin and 55 ml 0.15% hydroquinone. Slides were immersed in developer for up to 2 min, until black colouration of the tissue section was detected, then immersed in running hot tap water, rinsed in distilled water and incubated in 5% sodium thiosulfate (in acidulated water) for 2 min. Slides were rinsed in distilled water, dehydrated in a graded alcohol series and permanently mounted. Images were captured using a BX53 microscope and DP73 digital camera (Olympus, Southend-on-Sea, U.K.).

Image Analysis and Statistical testing

Assessment of FRM abundance was performed by calculating the percentage of positive immunofluorescence staining in the area of the papillary dermis and reticular dermis using ImageJ software (Abramoff et al., 2004). All resultant data is presented as mean ± SEM. Statistical analysis was performed using GraphPad Prism 7.01 (GraphPad Software, Inc. La Jolla, California, U.S.A.). Results were considered significant if $P < 0.05$ (95% confidence level). FRM length was calculated by counting the number of beads per microfibril and statistically tested using Mann-Whitney U test. FRM immunofluorescence abundance was tested using Student's t-test.

Regression modelling was conducted using Stata V15 software (StataCorp. 2017. *Stata Statistical Software: Release 15*. College Station, TX: StataCorp LLC) in order to determine whether differences in periodicity existed between the two groups, controlling for participant age and gender. As the data were hierarchical - inter-bead periodicity is 'clustered' within FRM which, themselves are clustered with participants - we initially fitted a multi-level mixed-effects linear regression model, which takes account of both the potential correlation between periodicity measurements within the same FRM and the potential correlation of FRMs within the same participant (although the latter is likely to be smaller). As the sample of periodicity measurements has some positive skew and is highly kurtotic, a non-parametric bootstrapped standard error was also derived, using 200 replications and a random initial-value 'seed'. Having run these models, it was apparent that there was some mis-specification, as there were inconsistencies in the estimated standard errors. We therefore decided to take account of the likely correlation between any randomly chosen periodicity measurement and its preceding one in the 'chain' (known as auto-regression). We therefore fitted separate population-averaged linear regression models, with auto-regressive order-1 correlations

(AR1) and robust standard errors (as bootstrapping is not available for this type of model), to the original data, to logarithmic-transformed data and to square root-transformed data.

RESULTS

Skin ethnicity influences the ultrastructure of adult FRMs

Photoprotected buttock skin biopsies were obtained from black African ("African") and white Northern European ("European") young adult volunteers. Buttock skin was selected as the anatomical site of interest as it is widely considered to be photoprotected; thus isolated FRMs should exhibit minimal photodamage. To confirm this, histological characterization of the biopsy samples was performed. Dual immunofluorescence staining for elastin and FRMs identified that the dermal elastic fibre network components were arranged in arborizing arrays connecting the oxytalan fibres of the DEJ to the elaunin fibres of the superficial papillary dermis (Figure 1a). In agreement with previous studies, FRMs were differentially deposited in the papillary dermis, with black African skin containing significantly more FRMs than white Northern European skin ($P < 0.001$); whilst in the reticular dermis, no difference in FRM distribution was identified between cohorts (Figure 1b). Importantly, there was no evidence of solar elastosis – the characteristic accumulation of dystrophic elastic material in the dermis due to prolonged and excessive sun exposure – in any of the skin biopsies studied. Furthermore, melanin distribution detected using the Warthin-Starry method (Figure 1c) confirmed that European buttock skin had minimal constitutive pigmentation and no evidence of facultative pigmentation – a finding consistent with these samples being obtained from photoprotected skin.

Next, FRMs were isolated from both superficial papillary and deeper reticular dermis of each biopsy and characterized using the ultrastructural parameters of bead number per FRM and inter-bead periodicity (Figure 2a). For the papillary dermis, the number of beads per FRM was not significantly different between African [median = 8.5; interquartile range (IQR; 8.0, 11.5)] and European [median = 9.0; IQR (8.5, 11.8)] cohorts. However, for the reticular dermis the number of beads per FRM, whilst not different from each other, were significantly increased compared to the papillary dermis for both cohorts [African: median = 17.0; IQR (15.0, 23.5); European: median = 18.5; IQR (16.8, 23.3); $P < 0.01$; Figure 2b].

Initial analysis of periodicity for FRM isolated from the papillary dermis suggested that there was no difference between ethnic groups (mean ± standard deviation [SD]; African: 55.13 ± 10.74 nm; European: 56.74 ± 11.92 nm). However, examination of the cumulative distributions revealed differences in their distributions (Figure 2c). Regardless of whether the original-, logarithmic- or square root-transformed data were used, periodicity was significantly larger in FRMs from European participants than from African participants. For ease of interpretation, we display here the original data. Controlling for age and gender, the difference in periodicity was 2.20 nm [95% C.I. (1.33 nm, 3.08 nm); $P<0.001$].

In contrast, the periodicity of FRMs extracted from the reticular dermis were invariant between ethnic groups (mean ± SD; African: 56.73 ± 12.37 nm; European: 56.59 ± 11.32 nm). Examination of the cumulative distributions (Figure 2d) and statistical modelling confirmed that reticular dermis FRMs were not significantly different between cohorts. Using the original data (both logarithmic- and square root-transformations did not alter the conclusions), there was no significant difference in average periodicity between European and African participants [difference = 0.69 nm; 95% C.I. (-0.37 nm, 1.74 nm); $P=0.202$].

These observations demonstrate that the reticular dermis of African and European subjects contains FRMs with invariant periodicity and length. However, the papillary dermis of both African and European subjects contained FRMs that were shorter than those resident in the reticular dermis. Furthermore, European papillary dermal FRMs displayed increased inter-bead periodicity as compared to those extracted from the papillary dermis of African skin (see Table 1 for summary of results).

Neonatal FRMs are ultrastructurally invariant

We next assessed whether these differences in FRM ultrastructure were present during early post-natal development by extracting FRMs from full-thickness neonatal foreskin. Histologic analysis of neonatal foreskin from African and European infants identified an abundance of dermal FRMs that were immunopositive for both fibrillin-1 and fibrillin-2 (Figure 3a). Analysis of FRMs isolated from these foreskin samples identified that the number of beads per microfibril was invariant between African [median = 7.0; IQR (6.0, 7.3)] and European [median = 7.0; IQR (6.0, 8.3); Figure 3b] infants. Similarly, analyses of FRM periodicity found no significant difference between neonatal cohorts (mean ± SD; African: 56.09 ± 13.56 nm; European: 55.94 ± 12.69 nm), a finding that was confirmed by regression modelling. Controlling for gender only, the average difference in periodicity between European and African neonates was -0.16 nm [95% C.I. (-1.97 nm, 1.66 nm), P=0.865]. This data suggests that at birth, FRMs extracted from full-thickness foreskin are invariant across ethnic groups and thus, the differences identified in FRMs extracted from the papillary dermis of adult photoprotected buttock may be acquired during the passage of time from childhood to mature adulthood. Alternatively, differences in papillary dermal FRMs may also exist at birth but

were not detected due to the extraction of FRMs from the entire dermis, rather than from each dermal layer, as was performed for adult skin.

DISCUSSION

In this study, we established that FRMs isolated from neonatal foreskin of African and European subjects were ultrastructurally invariant. However, in adult skin, dermal location had a profound impact on the ultrastructure of extracted FRMs; those from the reticular dermis contained twice the number of beads per microfibril as compared to those extracted from papillary dermis. Furthermore, reticular dermal FRMs had a more consistent inter-bead periodicity between ethnic cohorts. In contrast, photoprotected adult papillary dermal FRM exhibited marked differences in periodicity with those extracted from European skin, having a significantly increased periodicity compared to those of African subjects. Our data therefore suggests that although FRM from different ethnic groups are invariant in the neonatal period of life, the passage of time to adulthood impacts upon the ultrastructure of FRMs resident in the papillary dermis but not reticular dermis.

FRMs are evolutionarily highly conserved from jellyfish to man. In mammalian tissues, they appear structurally similar and retain a bead-like arrangement (Baldock et al., 2001). Here we demonstrate that during human foetal development, FRM synthesis appears invariant irrespective of ethnic background, a finding consistent with their highly conserved evolution. These neonatal foreskin FRMs comprised both fibrillin-1 and fibrillin-2 and may represent a naïve, structurally immature phenotype (Zhang et al., 1994, Zhang et al., 1995) – more akin to FRMs that are synthesized *in vitro* from human dermal fibroblasts (Hibbert et al., 2015). A potential limitation of these data is the assumption that neonatal foreskin represents a faithful model of adult photoprotected skin. Due to ethical constraints restricting obtaining neonatal photoprotected buttock skin via biopsy, foreskin represented an anatomical site that is both photoprotected and accessible due to its removal during routine circumcision. Furthermore, it

would have been preferable to dissect the foreskin into papillary and reticular layers; however, this was not achievable due to the thin and fragile nature of the tissue sample.

FRMs are present in a variety of human tissues and the different roles they play may be reflected in the structure they adopt. Here, we demonstrate that even within the same tissue - adult skin - the dermal location from which FRMs were extracted had a profound effect on the ultrastructure observed. Reticular dermal FRMs exhibited twice the number of beads per microfibril as compared to those extracted from papillary dermis. FRMs of the papillary and reticular dermis are likely to play very different architectural and mechanical roles within the skin. Anatomically, papillary dermal FRMs exist in an arrangement perpendicular to the DEJ and consist of either discrete bundles of oxytalan fibres or associated with elastin-containing elaunin fibres; whereas in the reticular dermis, FRMs decorate mature elastic fibres, i.e. coascervated elastin supported by FRM assemblies, that run parallel to the DEJ (Cotta-Pereira et al., 1976, Mithieux and Weiss, 2005). Differences in bead length may also arise as a result from the cell type from which they are derived; fibroblasts are thought to be principally responsible for FRM deposition in human skin (Long and Tranquillo, 2003). However, there are additional data that identify epidermal keratinocytes as also contributing to FRM synthesis *in vivo* (Haynes et al., 1997, Watson et al., 1999), particularly to the deposition of FRM in the papillary dermis. Recent data has highlighted the extent of fibroblast heterogeneity in human skin with at least four distinct fibroblast populations existing, not all of which are spatially segregated (Philippeos et al., 2018). It is therefore feasible that diverse cell types - fibroblasts *and* keratinocytes - are able to synthesize FRMs of variable bead length.

In common with other ECM assemblies, FRMs are thought to persist in skin for many years (Shapiro et al., 1991); as a consequence they are susceptible to gradual accumulation of damage. FRMs extracted from the papillary dermis of European subjects exhibited significant differences in periodicity compared to those of African subjects. These FRMs were extracted from buttock, which is widely considered to be a photoprotected anatomic site. Whilst we did not identify in our skin biopsies any characteristics of photodamage (such as solar elastosis or facultative pigmentation), papillary dermal FRMs have previously been shown to be particularly susceptible to photoexposure, due in part to their close proximity to the epidermis (Langton et al., 2017, Watson et al., 1999). Excessive sun exposure, mainly in childhood, and various high-risk activities, such as intentional sunbathing, inadequate sun protection and the use of tanning lamps (Cercato et al., 2013, Turrisi et al., 2006) could all induce skin damage in white Northern European individuals. In contrast, in highly pigmented black African skin the protection factor afforded by melanin in basal keratinocytes is estimated to be approximately 60 fold (Fajuyigbe et al., 2018). It is therefore possible that low level incidental irradiation may not impact the dermal layer of African skin and thus ultrastructural damage to African FRMs is largely prevented.

Oxidative stress induced by reactive oxygen species (ROS) may also mediate damage to ECM components (see review (Naidoo et al., 2018)). Human skin is exposed to ROS generated from both environmental sources such as sun exposure, airborne pollutants and particulate matter, as well as diet and endogenous oxidative metabolism (Vierkotter and Krutmann, 2012). Thus skin-derived FRMs may accumulate time-related damage through formation of oxidative cross-links induced by the long-term exposure to ROS (Wang et al., 2014) and also via the accrual of advanced-glycation end products on fibrillin-1 (Atanasova et al., 2009). More recently, it has been shown that UVA exposure can induce the release of

nitric oxide (NO) from skin (Liu et al., 2014). UVA-induced NO release from cutaneous stores can act systemically (Halliday and Byrne, 2014) with both protective (Liu et al., 2014) and toxic outcomes (Juzeniene et al., 2011). Feasibly the high constitutive pigmentation afforded by the distribution of melanin throughout all layers of the epidermis of black skin (Fajuyigbe et al., 2018) may prevent UV-induction of mediators such as ROS and NO at photoexposed anatomical sites, thus protecting against deleterious remodelling of the FRMs. Consequently, individuals with lower levels of constitutive protection, such as white Northern Europeans, may accrue systemic damage.

Conversely, it is possible that FRMS extracted from the papillary dermis of adult black African skin undergo a conformational change that causes a reduction to their interbead periodicity during the period of time to adulthood. This ultrastructural change may occur due to a selective evolutionary pressure to preserve FRMs from deleterious remodelling events. Changes to FRM interbead periodicity would likely arise during FRM assembly - a process that is not yet fully characterized but is proposed to follow either a hinged or staggered model (Kielty et al., 2005). During FRM assembly, both intra- and inter-molecular folding of fibrillins may alter interbead periodicity. Similarly, it is within the interbead region that the alignment of fibrillin molecules is defined by transglutaminase-derived cross-links (Qian and Glanville, 1997). Thus, both folding and cross-linking events may affect the structural organization of FRMs and, as a consequence, alter their susceptibility to damage.

Fibrillin microfibril and elastic fibre biology is highly complex. Such complexity presents a technical challenge in unravelling the multiple molecular interactions that FRMs possess. Proteomic analysis such as mass spectrometry has the potential to identify a large number of molecules that colocalize or interact with FRMs (for a review see (Thomson et al., 2019)).

Although beyond the scope of the current manuscript, future studies could focus on understanding the precise molecular composition of FRMs isolated from individuals of diverse ancestry. More importantly, the accessibility of skin makes this an exceptionally useful tissue to examine the role of FRMs and to translate these findings into other FRM-rich tissues such as blood vessels, lung and ocular ligaments. Understanding how FRMs play their key role in tissue homeostasis through their interaction with growth factors such as transforming growth factor-β (TGFβ) and bone morphogenetic proteins (BMPs), and through interaction with cell surface receptors such as the integrins (Bax et al., 2003) and syndecans (Bax et al., 2007) becomes a realistic possibility through the study of skin. This provides a clear future opportunity to intervene in, and to recognize disease processes and mechanisms of ageing, and to control tissue development for tissue engineering applications. Furthermore, previously unappreciated differences in skin-derived FRMs from diverse ethnic cohorts may indicate that other FRM-rich tissues will have similar ethnicity-related differences. Regardless of the causative mechanism underpinning these ultrastructural differences in skin-derived FRMs, such alterations are likely to lead to profound biomechanical and biochemical consequences to skin function and health.

ACKNOWLEDGEMENTS

We are grateful for the technical assistance of Dr Nigel Hodson from The University of Manchester BioAFM Facility. Professor Chris Griffiths is an NIHR Senior Investigator. Professor Griffiths and Professor Rachel Watson are supported in part by the NIHR Manchester Biomedical Research Centre. This study was funded by a programme grant from Walgreens Boots Alliance.

AUTHOR CONTRIBUTIONS

AKL, MJS and REBW designed the research. SSAC, AC and SK provided tissue samples. AKL, PC and PH, SSAC performed the experiments and acquired data. AKL and MH statistically analyzed the data. AKL, MH, CEMG and REBW wrote the manuscript.

REFERENCES

ABRAMOFF, M. D., MAGELHAES, P. J. & RAM, S. J. 2004. Image processing with ImageJ. *Biophotonics International,* 11**,** 36-42.

AFZAL, U., WATSON, R. E. B. & LANGTON, A. K. 2017. Cover Image: Capturing the architectural beauty of the dermal elastic fibre network. *Br J Dermatol,* 177**,** 1141-1142.

ATANASOVA, M., KONOVA, E., BETOVA, T. & BAYDANOFF, S. 2009. Non-Enzymatic Glycation of Human Fibrillin-1. *Gerontology,* 55**,** 73-81.

BALDOCK, C., KOSTER, A. J., ZIESE, U., et al. 2001. The supramolecular organization of fibrillin-rich microfibrils. *J Cell Biol,* 152**,** 1045-56.

BAX, D. V., BERNARD, S. E., LOMAS, A., et al. 2003. Cell adhesion to fibrillin-1 molecules and microfibrils is mediated by alpha 5 beta 1 and alpha v beta 3 integrins. *J Biol Chem,* 278**,** 34605-16.

BAX, D. V., MAHALINGAM, Y., CAIN, S., et al. 2007. Cell adhesion to fibrillin-1: identification of an Arg-Gly-Asp-dependent synergy region and a heparin-binding site that regulates focal adhesion formation. *J Cell Sci,* 120**,** 1383-92.

CERCATO, M. C., NAGORE, E., RAMAZZOTTI, V., SPERDUTI, I. & GUILLEN, C. 2013. Improving sun-safe knowledge, attitude and behaviour in parents of primary school children: a pilot study. *J Cancer Educ,* 28**,** 151-7.

COTTA-PEREIRA, G., GUERRA RODRIGO, F. & BITTENCOURT-SAMPAIO, S. 1976. Oxytalan, elaunin, and elastic fibers in the human skin. *J Invest Dermatol,* 66**,** 143-8.

ECKERSLEY, A., MELLODY, K. T., PILKINGTON, S., et al. 2018. Structural and compositional diversity of fibrillin microfibrils in human tissues. *J Biol Chem,* 293**,** 5117-5133.

EDWARDS, C. & MARKS, R. 1995. Evaluation of biomechanical properties of human skin. *Clin Dermatol,* 13**,** 375-80.

FAJUYIGBE, D., LWIN, S. M., DIFFEY, B. L., et al. 2018. Melanin distribution in human epidermis affords localized protection against DNA photodamage and concurs with skin cancer incidence difference in extreme phototypes. *FASEB J***,** fj201701472R.

GIRARDEAU-HUBERT, S., PAGEON, H. & ASSELINEAU, D. 2012. In vivo and in vitro approaches in understanding the differences between Caucasian and African skin types: specific involvement of the papillary dermis. *Int J Dermatol,* 51 Suppl 1**,** 1-4.

GIRARDEAU, S., MINE, S., PAGEON, H. & ASSELINEAU, D. 2009. The Caucasian and African skin types differ morphologically and functionally in their dermal component. *Exp Dermatol,* 18**,** 704-11.

HALLIDAY, G. M. & BYRNE, S. N. 2014. An unexpected role: UVA-induced release of nitric oxide from skin may have unexpected health benefits. *J Invest Dermatol,* 134**,** 1791-1794.

HAYNES, S. L., SHUTTLEWORTH, C. A. & KIELTY, C. M. 1997. Keratinocytes express fibrillin and assemble microfibrils: implications for dermal matrix organization. *Br J Dermatol,* 137**,** 17-23.

HIBBERT, S. A., WATSON, R. E. B., GIBBS, N. K., et al. 2015. A potential role for endogenous proteins as sacrificial sunscreens and antioxidants in human tissues. *Redox Biol,* 5**,** 101-13.

HUSSAIN, S. H., LIMTHONGKUL, B. & HUMPHREYS, T. R. 2013. The Biomechanical Properties of the Skin. *Dermatologic Surgery,* 39**,** 193-203.

JOLY-TONETTI, N., WIBAWA, J. I., BELL, M. & TOBIN, D. 2016. Melanin fate in the human epidermis: a reassessment of how best to detect and analyse histologically. *Exp Dermatol,* 25**,** 501-4.

JUZENIENE, A., MA, L. W., KWITNIEWSKI, M., et al. 2011. Influenza, Solar Radiation and Vitamin D. *Anticancer Research,* 31**,** 1502-1502.

KEENE, D. R., MADDOX, B. K., KUO, H. J., SAKAI, L. Y. & GLANVILLE, R. W. 1991. Extraction of extendable beaded structures and their identification as fibrillin-containing extracellular matrix microfibrils. *J Histochem Cytochem,* 39**,** 441-9.

KIELTY, C. M., SHERRATT, M. J., MARSON, A. & BALDOCK, C. 2005. Fibrillin microfibrils. *Adv Protein Chem,* 70**,** 405-36.

KIELTY, C. M., SHERRATT, M. J. & SHUTTLEWORTH, C. A. 2002. Elastic fibres. *J Cell Sci,* 115**,** 2817-28.
LANGTON, A. K., ALESSI, S., HANN, M., et al. 2019a. Aging in Skin of Color: Disruption to Elastic Fiber Organization Is Detrimental to Skin's Biomechanical Function. *J Invest Dermatol,* 139**,** 779-788.
LANGTON, A. K., GRAHAM, H. K., GRIFFITHS, C. E. M. & WATSON, R. E. B. 2019b. Ageing significantly impacts the biomechanical function and structural composition of skin. *Exp Dermatol,* 28**,** 981-984.
LANGTON, A. K., GRAHAM, H. K., MCCONNELL, J. C., et al. 2017. Organization of the dermal matrix impacts the biomechanical properties of skin. *Br J Dermatol,* 177**,** 818-827.
LANGTON, A. K., SHERRATT, M. J., SELLERS, W. I., GRIFFITHS, C. E. M. & WATSON, R. E. B. 2014. Geographical ancestry is a key determinant of epidermal morphology and dermal composition. *Br J Dermatol,* 171**,** 274-82.
LIU, D., FERNANDEZ, B. O., HAMILTON, A., et al. 2014. UVA irradiation of human skin vasodilates arterial vasculature and lowers blood pressure independently of nitric oxide synthase. *J Invest Dermatol,* 134**,** 1839-1846.
LONG, J. L. & TRANQUILLO, R. T. 2003. Elastic fiber production in cardiovascular tissue-equivalents. *Matrix Biology,* 22**,** 339-350.
MITHIEUX, S. M. & WEISS, A. S. 2005. Elastin. *Adv Protein Chem,* 70**,** 437-61.
NAIDOO, K., HANNA, R. & BIRCH-MACHIN, M. A. 2018. What is the role of mitochondrial dysfunction in skin photoaging? *Exp Dermatol,* 27**,** 124-128.
PHILIPPEOS, C., TELERMAN, S. B., OULES, B., et al. 2018. Spatial and Single-Cell Transcriptional Profiling Identifies Functionally Distinct Human Dermal Fibroblast Subpopulations. *Journal of Investigative Dermatology,* 138**,** 811-825.
QIAN, R. Q. & GLANVILLE, R. W. 1997. Alignment of fibrillin molecules in elastic microfibrils is defined by transglutaminase-derived cross-links. *Biochemistry,* 36**,** 15841-7.
SHAPIRO, S. D., ENDICOTT, S. K., PROVINCE, M. A., PIERCE, J. A. & CAMPBELL, E. J. 1991. Marked longevity of human lung parenchymal elastic fibers deduced from prevalence of D-aspartate and nuclear weapons-related radiocarbon. *J Clin Invest,* 87**,** 1828-34.
SHERRATT, M. J., BAYLEY, C. P., REILLY, S. M., et al. 2010. Low-dose ultraviolet radiation selectively degrades chromophore-rich extracellular matrix components. *J Pathol,* 222**,** 32-40.
THOMSON, J., SINGH, M., ECKERSLEY, A., et al. 2019. Fibrillin microfibrils and elastic fibre proteins: Functional interactions and extracellular regulation of growth factors. *Semin Cell Dev Biol,* 89**,** 109-117.
TURRISI, R., HILLHOUSE, J., ROBINSON, J., STAPLETON, J. & ADAMS, M. 2006. Influence of parent and child characteristics on a parent-based intervention to reduce unsafe sun practices in children 9 to 12 years old. *Arch Dermatol,* 142**,** 1009-14.
VIERKOTTER, A. & KRUTMANN, J. 2012. Environmental influences on skin aging and ethnic-specific manifestations. *Dermatoendocrinol,* 4**,** 227-31.
WANG, Z., LYONS, B., TRUSCOTT, R. J. W. & SCHEY, K. L. 2014. Human protein aging: modification and crosslinking through dehydroalanine and dehydrobutyrine intermediates. *Aging Cell,* 13**,** 226-234.
WATSON, R. E. B., GRIFFITHS, C. E. M., CRAVEN, N. M., SHUTTLEWORTH, C. A. & KIELTY, C. M. 1999. Fibrillin-rich microfibrils are reduced in photoaged skin. Distribution at the dermal-epidermal junction. *J Invest Dermatol,* 112**,** 782-7.
ZHANG, H., APFELROTH, S. D., HU, W., et al. 1994. Structure and expression of fibrillin-2, a novel microfibrillar component preferentially located in elastic matrices. *J Cell Biol,* 124**,** 855-63.
ZHANG, H., HU, W. & RAMIREZ, F. 1995. Developmental expression of fibrillin genes suggests heterogeneity of extracellular microfibrils. *J Cell Biol,* 129**,** 1165-76.

Table 1. Interbead periodicity values for black African and white Northern European individuals

	African	Northern European	Significance
Foreskin periodicity (mean ± SD [nm])	56.09 ± 13.56	55.94 ± 12.69	P = 0.865
Papillary dermis periodicity (mean ± SD [nm])	55.13 ± 10.74	56.74 ± 11.92	P < 0.001
Reticular dermis periodicity (mean ± SD [nm])	56.73 ± 12.37	56.59 ± 11.32	P = 0.202

FIGURE LEGENDS

Figure 1. Histologic characteristics of photoprotected adult skin

Dual immunofluorescence staining for elastin and FRMs identified that dermal elastic fiber network components were arranged in arborizing arrays connecting the oxytalan fibers of the DEJ to the elaunin fibers of the superficial papillary dermis (**a**). Image analysis revealed FRMs of the papillary dermis are significantly reduced in Northern European skin as compared to black African skin; however, this difference is not apparent in the reticular dermis (**b**). Red = fibrillin, green = elastin, blue = DAPI. Scale bar = 50 μm Melanin distribution detected using the Warthin-Starry method confirmed that white Northern European photoprotected buttock skin had minimal constitutive pigmentation and no evidence of facultative pigmentation (**c**). Scale bar: 50 μm.

Figure 2. Skin ethnicity influences the periodicity of adult FRMs

(**a**) Experimental isolation of FRMs from the papillary dermis of adult buttock skin was performed by cryosectioning bisected 6 mm skin biopsies *en face* to a depth of 400 μm. The next 100 μm was cryosectioned from the skin biopsy and discarded. Reticular dermis FRMs were then isolated from the remaining skin biopsy. Scale bar: 100 μm. Representative atomic force microscopy (AFM) images of FRM isolated from human papillary and reticular dermis reveal the "beads-on-a-string" morphology. Measurement of the inter-bead region provides a measure of FRM ultrastructure termed periodicity. Scale bar = 200 nm. (**b**) The number of beads per FRM was significantly increased in the reticular dermis, as compared to the papillary dermis for both cohorts. Cumulative frequency plots of inter-bead periodicity for FRMs isolated from photoprotected skin biopsies from adult individuals identifies significant differences between the ethnic cohorts for the papillary dermis (**c**) but not the reticular dermis (**d**).

Figure 3. FRMs isolated from neonatal foreskins have invariant ultrastructure

Immunofluorescence staining of neonatal foreskin revealed an abundance of FRMs which were immunopositive for fibrillin-1 and the perinatal isoform, fibrillin-2 (a). Scale bar = 50 μm. Ultrastructural characterization of FRMs isolated from neonatal foreskin revealed no significant difference in the number of beads per FRM (**b**) or inter-bead periodicity (**c**) between cohorts.

Figure 1

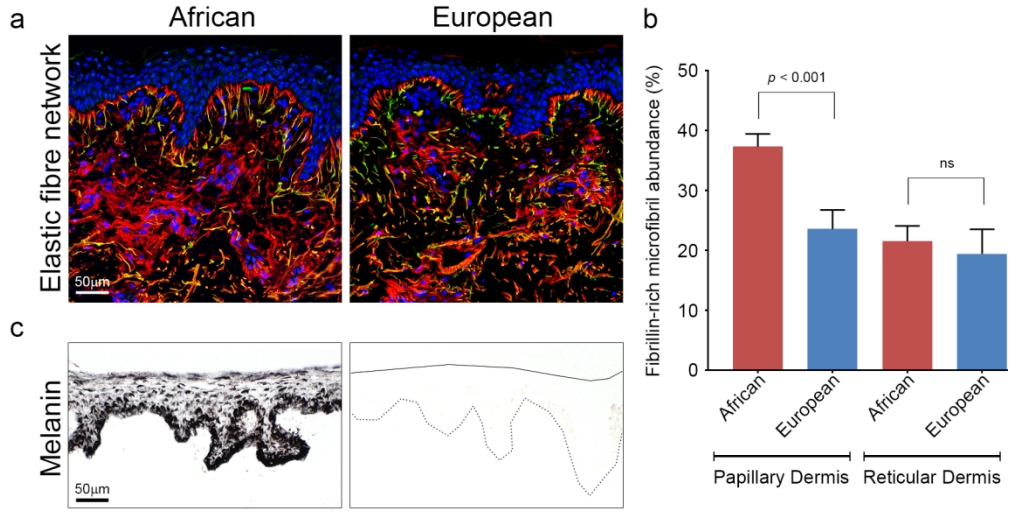

Figure 1. Histologic characteristics of photoprotected adult skin
Dual immunofluorescence staining for elastin and FRMs identified that dermal elastic fiber network components were arranged in arborizing arrays connecting the oxytalan fibers of the DEJ to the elaunin fibers of the superficial papillary dermis (a). Image analysis revealed FRMs of the papillary dermis are significantly reduced in Northern European skin as compared to black African skin; however, this difference is not apparent in the reticular dermis (b). Red = fibrillin, green = elastin, blue = DAPI. Scale bar = 50 µm
Melanin distribution detected using the Warthin-Starry method confirmed that white Northern European photoprotected buttock skin had minimal constitutive pigmentation and no evidence of facultative pigmentation (c). Scale bar: 50 µm.

Figure 2

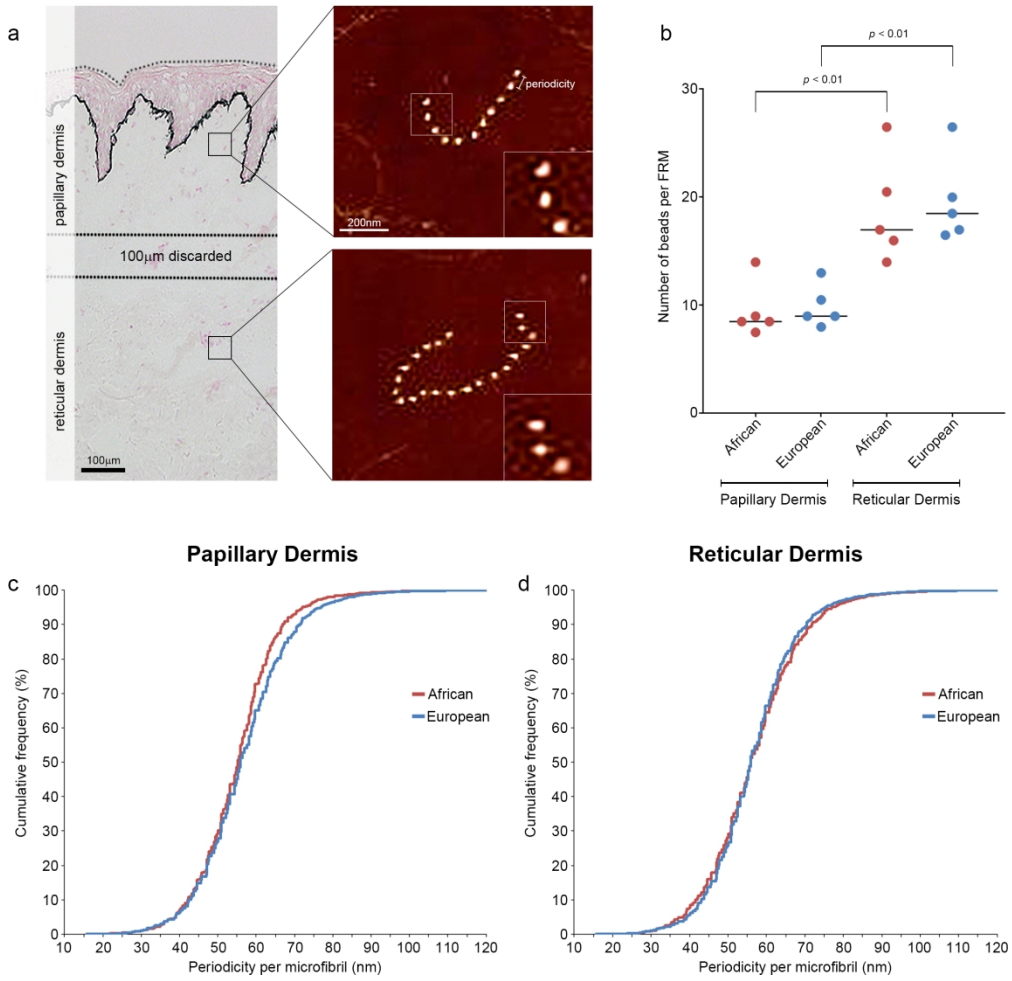

Figure 2. Skin ethnicity influences the periodicity of adult FRMs
(a) Experimental isolation of FRMs from the papillary dermis of adult buttock skin was performed by cryosectioning bisected 6 mm skin biopsies en face to a depth of 400 μm. The next 100 μm was cryosectioned from the skin biopsy and discarded. Reticular dermis FRMs were then isolated from the remaining skin biopsy. Scale bar: 100 μm. Representative atomic force microscopy (AFM) images of FRM isolated from human papillary and reticular dermis reveal the "beads-on-a-string" morphology. Measurement of the inter-bead region provides a measure of FRM ultrastructure termed periodicity. Scale bar = 200 nm. (b) The number of beads per FRM was significantly increased in the reticular dermis, as compared to the papillary dermis for both cohorts. Cumulative frequency plots of inter-bead periodicity for FRMs isolated from photoprotected skin biopsies from adult individuals identifies significant differences between the ethnic cohorts for the papillary dermis (c) but not the reticular dermis (d).

Figure 3

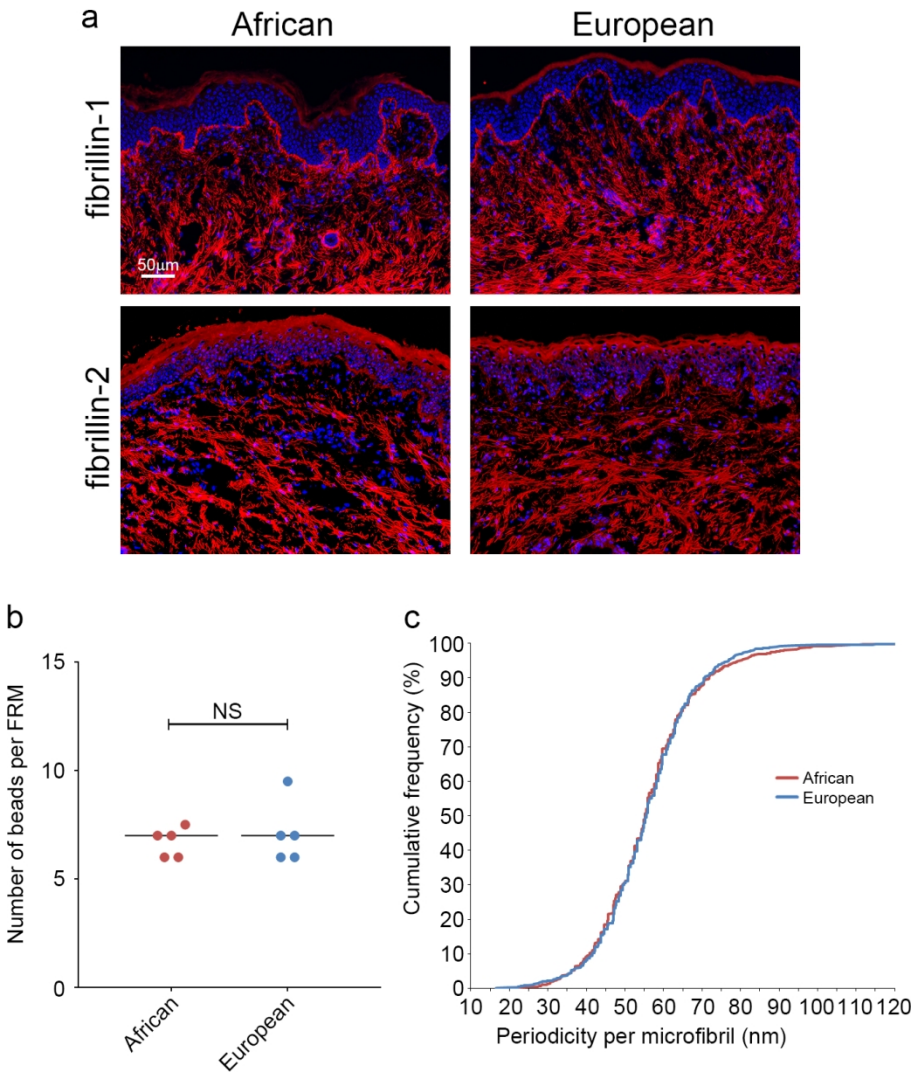

Figure 3. FRMs isolated from neonatal foreskins have invariant ultrastructure
Immunofluorescence staining of neonatal foreskin revealed an abundance of FRMs which were immunopositive for fibrillin-1 and the perinatal isoform, fibrillin-2 (a). Scale bar = 50 μm. Ultrastructural characterization of FRMs isolated from neonatal foreskin revealed no significant difference in the number of beads per FRM (b) or inter-bead periodicity (c) between cohorts.